Plasmon Oscillations and de Broglie's Matter Waves Instabilities

M. Akbari-Moghanjoughi[1]

[1]*Faculty of Sciences, Department of Physics,*

Azarbaijan Shahid Madani University, 51745-406 Tabriz, Iran

(Dated: February 13, 2020)

Abstract

In this research we study the effect of matter wave instability on propagation of electron beam with arbitrary degree of degeneracy. Particular class of solutions of the Schrödinger-Poisson system is used to model the electron-beam propagation. It is shown that the electron-beam propagating at a constant average speed is described by a coupled driven pseudoforce system solution of which leads to plasmon excitations with dual wave-particle character. The fundamental quantum mechanical de Broglie relation is found to be due to the resonant interaction of particle-like plasmon excitation branch with the electron beam drift. We further obtain a generalized double lengthscale de Broglie wave-particle relation through which various beam-plasmon instability is studied in this model. The effects of charge screening and periodic lattice structure on the matter wave interaction and instabilities are discussed. Current research may further illuminate the origin of matter wave in quantum mechanics and may lead to clear understanding of novel wave-particle interactions.

PACS numbers: 52.30.-q,71.10.Ca, 05.30.-d

I. INTRODUCTION

Plasma oscillations play fundamental role in many physical phenomena associated with collective interaction of charged species. Due to complex nature of electromagnetic interactions between variety of charges in multispecies plasmas a wide spectrum of interesting linear and nonlinear phenomena such as different instabilities [1], wave-particle interaction [2], solitons, double layer, shock waves [3], etc. can exist in these environments. Plasma theories such a kinetic and hydrodynamic models have been developed over the past decade in order to study various interesting collective effects [4–7]. In plasmas the electron fluid is almost the main ingredient of dielectric response to electromagnetic waves and dynamic structure factor [8–11] leading to many interesting phenomena such as Thomson, Compton [12–14], stimulated Raman and Brillouin [15, 16] scattering which are used as efficient plasma diagnostic tools. Electrons are also responsible for other important physical properties of plasmas such as charge shielding [17–23], ionic bound states [24–33], electrical and energy transport phenomena, heat capacity [34] and many others. Dielectric response of electron gas in solid state plasmas plays the prominent role in optical properties of metals [35, 36], semiconductors [37, 38], nanometallic structures, low dimensional system and liquid crystals [39–45]. However, in order to understand many of the physical properties of plasmas one has to have detailed information on collective aspects of electron species in these environments. In hydrodynamic plasma theories the electron dynamic is simply coupled to electromagnetic fields through Maxwell equations. Therefore, hydrodynamic and magnetohydrodynamic theories constitute a cost effective and analytic means to investigate a wide range of plasma phenomena in a straightforward manner [46]. These theories, if properly formulated, are also believed to be able to capture many collective aspect such as collisionless or collisional damping previously known to be purely kinetic effects [47].

Due to evergrowing necessity of developments in miniaturized low-dimensional, semiconductor and nanostructured devices for futuristic electronic purposes, a renewed effort has been devoted to discover physical properties of dense quantum electron gas over the past few years. Although the theories of collective quantum electron gas dielectric response has been fully developed more than half a century ago [48–61], many interesting properties of quantum electron fluid is yet to be discovered. Many renewed and enhanced quantum kinetic and quantum hydrodynamic theories have emerged over the recent years. Application

of these theories predicts a very insightful future for the science of quantum plasmas and have helped to discover a broad range of new interesting collective phenomena of quantum electron gas unknown up until the recent decade [62–73]. Application of Schrödinger-Poisson system [74] and coupled pseudoforce method has shown a dualtone wave- and particle-like dynamics of the quantum electron gas in a unique picture [75–81]. We strongly believe that this dual-lengthscale theory of quantum plasmas provides a better picture for wave-particle phenomena in collective environments such as plasmas and fluids. The quantum fluid theory may also provide appropriate answer to some of the most fundamental quantum mechanical questions regarding the matter waves and mysterious duality nature of particles [82] and nonlocality effect [83]. It has been recently shown that the Bohmian mechanics and the quantum potential appearing in the hydrodynamic formulations is more fundamental than the single-particle Schrödinger equation [84]. It has been therefore concluded that the Bohm's quantum potential makes a basis for the Schrödinger equation instead of being a consequence of this equation. Therefore, the proof of de Broglie's hypothetical matter wave relation given in current research is original in the sense that it does not rely on the fundamental equation of the quantum mechanics.

In current research starting from quantum hydrodynamic theory of an electron gas a one dimensional model of pseudoforce for arbitrary degenerate electron beam is developed and the de Broglie's hypothetical matter wave equation is mathematically described as a pseudoresonance effect between the particle-like branch of the plasmon excitation in the beam and the electron drift. A generalized dual wavenumber de Broglie equation is obtained which reduces to the original equation the classical dilute electron beam limit. Some interesting spatial matter wave instability in the beam propagation is introduced for the first time and discussed in terms of the average beam speed and electron screening effect.

II. MATHEMATICAL MODEL

Dynamic properties of a free electron gas can be studied through the hydrodynamic model to a great extent. Quantum hydrodynamic model may be used to study the dynamic properties of electron gas with arbitrary degree of degeneracy. A closed set of conventional

quantum hydrodynamic equations for isothermal electron gas read

$$\frac{\partial n}{\partial t}+\frac{\partial nv}{\partial x}=0, \tag{1a}$$

$$\frac{\partial v}{\partial t}+v\frac{\partial v}{\partial x}=\frac{e}{m}\frac{\partial \phi}{\partial x}-\frac{1}{m}\frac{\partial \mu}{\partial x}+\frac{\hbar^2}{2m^2}\frac{\partial}{\partial x}\left(\frac{1}{\sqrt{n}}\frac{\partial^2\sqrt{n}}{\partial x^2}\right), \tag{1b}$$

$$\frac{\partial^2\phi}{\partial x^2}=4\pi e\left(n-n_0\right), \tag{1c}$$

where the dependent variables n, v, μ and ϕ refer to the number density, average speed, chemical potential and electrostatic potential, respectively. The last term in the momentum equation is due to the Bohm potential which is the origin of nonlocal effects in de Broglie-Bohm pilot wave theory [83]. The parametric equation of state (EoS) for isothermal electron gas with arbitrary degree of nonrelativistic degeneracy is given in terms of the Fermi integrals

$$n(\eta,T)=\frac{2^{7/2}\pi m^{3/2}}{h^3}F_{1/2}(\eta)=-\frac{2^{5/2}(\pi m k_B T)^{3/2}}{h^3}\mathrm{Li}_{3/2}[-\exp(\eta)], \tag{2a}$$

$$P(\eta,T)=\frac{2^{9/2}\pi m^{3/2}}{3h^3}F_{3/2}(\eta)=-\frac{2^{5/2}(\pi m k_B T)^{3/2}(k_B T)}{h^3}\mathrm{Li}_{5/2}[-\exp(\eta)], \tag{2b}$$

where $\eta=\beta\mu$ with $\beta=1/k_BT$ and F_k is the Fermi integral of order k

$$F_k(\eta)=\int_0^\infty \frac{x^k}{\exp(x-\eta)+1}dx. \tag{3}$$

The function Li_k is called the polylog function defined as

$$F_k(\eta)=-\Gamma(k+1)\mathrm{Li}_{k+1}[-\exp(\eta)], \tag{4}$$

in which Γ is the gamma function. Note that the isothermal EoS is not the only choice and for fast processes the adiabatic EoS [23] may be employed. However, for illustrative simplified purpose we have chosen to use the isothermal electron EoS in current model. It is well known that the quantum hydrodynamic model (1) can be easily transformed [74] to the following Schrödinger-Poisson system using the Madelung transformations [48]

$$i\hbar\frac{\partial \mathcal{N}}{\partial t}=-\frac{\hbar^2}{2m}\frac{\partial^2\mathcal{N}}{\partial x^2}-e\phi\mathcal{N}+V_0\mathcal{N}+\mu(n,T)\mathcal{N}, \tag{5a}$$

$$\frac{\partial^2\phi}{\partial x^2}=4\pi e(|\mathcal{N}|^2-n_0), \tag{5b}$$

where $\mathcal{N}=\sqrt{n(x,t)}\exp[iS(x,t)/\hbar]$ is the state function characterizing spatiotemporal evolution of the electron gas with $\mathcal{N}\mathcal{N}^*=n(x,t)$ being the number density and $v(x,t)=$

$(1/m)\partial S(x,t)/\partial x$ the electron fluid speed. Also, V_0 represents a constant ambient potential. The coupled system (5) can be used to study the propagation of an electron beam of arbitrary degeneracy with arbitrary degree of degeneracy in an equilibrium temperature. Let us consider a beam of electron moving with a constant average speed, v through an electron gas with the chemical potential μ. The value of chemical potential varies depending the degeneracy degree of electron fluid. In the classical limit it can have the negative values up to zero electronvolts for dilute electron gas and positive few electronvolts for typical metals. Therefore, Schrödinger-Poisson system (5) can model a wide range of phenomenon for electron gas of arbitrary degeneracy. For our homogenous beam of electron gas moving with constant speed v one arrives at $S(x,t) = px + f(t)$ in which $p = mv$ is the average beam momentum and $f(t)$ is an arbitrary function of time. Therefore, the state function reduces to $\mathcal{N}(x,t) = \psi(x,t)\exp(ipx/\hbar)$ where $\psi(x,t) = \sqrt{n(x,t)}\exp[if(t)/\hbar]$.

To this end, let us now consider separable solution $\mathcal{N}(x,t) = \mathcal{R}(x)\mathcal{T}(t)$. After decoupling of spatial and temporal parts of first equation in (5), we find

$$\frac{\hbar^2}{2m}\frac{\partial^2\mathcal{R}(x)}{\partial x^2} + e\phi(x)\mathcal{R}(x) + [\epsilon - \mu(n,T)]\,\mathcal{R}(x) = V_0\mathcal{R}(x), \tag{6a}$$

$$\frac{\partial^2\phi(x)}{\partial x^2} = 4\pi e(|\mathcal{R}(x)|^2 - n_0), \tag{6b}$$

$$i\hbar\frac{\partial\mathcal{T}(t)}{\partial t} = \epsilon\mathcal{T}(t), \tag{6c}$$

where ϵ is the energy eigenvalue of the electronic system, $\mathcal{R}(x) = \sqrt{n(x)}\exp(ipx/\hbar)$ and $\mathcal{T}(t) = \sqrt{n(t)}\exp[if(t)/\hbar]$. The equation (6c) immediately leads to the solution $n(t) = \exp\{-2i[\epsilon t + f(t)]/\hbar\}$. Here we want to find the solution for spatial part, hence, the first two equations in (6) are our first concern. The linear system for small perturbations is [75]

$$\frac{\partial^2\Psi(x)}{\partial x^2} + \Phi(x) + 2E\Psi(x) = U_0\exp(ik_dx), \tag{7a}$$

$$\frac{\partial^2\Phi(x)}{\partial x^2} - \Psi(x) = 0, \tag{7b}$$

where μ_0 is the equilibrium constant chemical potential at $x = 0$ and $E = (\epsilon - \mu_0)/2E_p$ with $E_p = \hbar\omega_p$ being the plasmon energy and $\omega_p = \sqrt{4\pi e^2 n_0/m}$ the electron plasma frequency. We have also used the normalization scheme $\Psi(x) = \mathcal{R}(x)/\mathcal{R}(0)$ ($\mathcal{R}(0) = \sqrt{n_0}$ is the value of $\mathcal{R}(x)$ at $x = 0$), $\Phi(x) = e\phi/E_p$ and $U_0 = V_0/E_p$. The space coordinate x is normalized to the plasmon wavelength $\lambda_p = 2\pi/k_p$ with $k_p = \sqrt{2mE_p}/\hbar$ being the characteristic plasmon wavenumber. The parameter $k_d = p/\hbar k_p$ is the normalized de Broglie's matter wavenumber

which is to play a central role in this research. Note that we have further linearized the potential component leading to the important term $V_0 R(0)\exp(ipx/\hbar)$ which plays the role of a driving pseudoforce in the coupled linear differential system (7).

III. THE PSEUDORESONANCE EFFECT

In order to elucidate correspondence to the single particle quantum effect, we consider the particular case of $\Phi = U_0 = 0$. Then, we have in dimensional form

$$\frac{\partial^2\Psi(x)}{\partial x^2} + k^2\Psi(x) = 0, \quad k = \frac{\sqrt{2m(\epsilon-\mu_0)}}{\hbar}. \tag{8}$$

The solution to this equation is $\Psi(x) = \Psi_0\cos(kx)$ with tentative boundary conditions $\Psi(0) = \Psi_0$ and $\Psi'(0) = 0$, which reduces to the free particle wavefunction in the limit of dilute gas $\mu_0 \to 0$ with ϵ being particle energy. However, the fundamental relation between the particle momentum $p = mv$ and the wavenumber k has been hypothesized by de Broglie [85]. The later can be more clarified if we consider the driven pseudoforce equation

$$\frac{\partial^2\Psi(x)}{\partial x^2} + k^2\Psi(x) = k_0^2\cos(px/\hbar), \quad k_0 = \frac{\sqrt{2mV_0}}{\hbar}, \tag{9}$$

in which we have taken the real part of the potential energy, for illustration purpose. The pseudoresonant solution with the boundary conditions $\Psi(0) = \Psi'(0) = 0$ reads

$$\Psi(x) = \frac{k_0^2\left[\cos(kx) - \cos(px/\hbar)\right]}{p^2/\hbar^2 - k^2}. \tag{10}$$

And here comes the particle-beam momentum into the picture. Note that the solution (10) has the principal amplitude at the resonant point, $p = \pm\hbar k$, hence, the de Broglie's relation. In the dilute beam limit $\mu_0 \to 0$ one obtains the single particle parabolic energy dispersion $\epsilon = \hbar^2k^2/2m$. However, in the limit $p = \pm\hbar k$ the solution (10) becomes problematic.

Let us now go back to the normalized system (7) with real part of potential energy

$$\frac{\partial^2\Psi(x)}{\partial x^2} + \Phi(x) + 2E\Psi(x) = U_0\cos(k_d x), \tag{11a}$$

$$\frac{\partial^2\Phi(x)}{\partial x^2} - \Psi(x) = 0, \tag{11b}$$

The system (11) has the following solution for the boundary condition $\Phi(0) = \Phi_0$, $\Psi(0) = \Psi_0$

and $\Phi'(0) = \Psi'(0) = 0$

$$\Phi(x) = \Phi_g + \frac{U_0\left[(k_d^2 - k_1^2)\cos(k_2 x) - (k_d^2 - k_2^2)\cos(k_1 x) - 2\alpha\cos(k_d x)\right]}{2\alpha\,(k_d^2 - k_1^2)\,(k_d^2 - k_2^2)}, \tag{12a}$$

$$\Psi(x) = \Psi_g + \frac{U_0\left[(1 - k_d^2 k_1^2)\cos(k_1 x) - (1 - k_d^2 k_2^2)\cos(k_2 x) - 2\alpha k_d^2\cos(k_d x)\right]}{2\alpha\,(k_d^2 - k_1^2)\,(k_d^2 - k_2^2)}. \tag{12b}$$

where the general solutions $\Phi_g(x)$ and $\Psi_g(x)$ are

$$\begin{bmatrix} \Phi_g(x) \\ \Psi_g(x) \end{bmatrix} = \frac{1}{2\alpha}\begin{bmatrix} \Psi_0 + k_2^2\Phi_0 & -(\Psi_0 + k_1^2\Phi_0) \\ -(\Phi_0 + k_1^2\Psi_0) & \Phi_0 + k_2^2\Psi_0 \end{bmatrix}\begin{bmatrix} \cos(k_1 x) \\ \cos(k_2 x) \end{bmatrix}, \tag{13}$$

in which the dual characteristic wavenumbers k_1 and k_2 are given as

$$k_1 = \sqrt{E - \alpha}, \quad k_2 = \sqrt{E + \alpha}, \quad \alpha = \sqrt{E^2 - 1}. \tag{14}$$

The characteristic wavenumbers satisfy complementarity-like relation $k_1 k_2 = 1$. It is interesting to see that solutions (12) are doubly resonant at $k_1 = k_d$ and $k_2 = k_d$ where the wavenumber k_1 and k_2, respectively, characterize the wave-like and particle-like behavior of the electron beam propagation. The plasmon wavenumbers lead to a generalized energy dispersion of $E = (1 + k^4)/2k^2$ where E and k are scaled in terms of E_p and k_p, respectively. This dispersion is graphically compared to the single particle one in Fig. 1(a). The two wave and particle branches meet each other at the quantum beating point $k = k_p$. The particle branch of plasmon energy dispersion curve asymptotically approaches that of the single particle one at very higher energies. There is also an energy gap below the critical $E_{cr} = E_p$ which vanishes at the limit $\mu_0 \to 0$.

Assuming the average energy eigenvalue for electrons in the beam as $\epsilon = p^2/2m$ and using the generalized plasmon energy dispersion, we arrive at the generalized de Broglie relation $k_{1,2} = \sqrt{(\gamma^2 - \mu)/2 \mp \sqrt{(\gamma^2 - \mu)^2/4 - 1}}$ in which the wave and particle wavenumbers correspond respectively to the minus and plus signs. Also, $\gamma = v/v_d$ with $v_d = \sqrt{2E_p/m}$ being the plasmon velocity and $\mu = \mu_0/2E_p$ is the normalized chemical potential. Note that in the limit $\mu_0 \ll 2E_p$ for dilute beam and $v \gg v_p$ for particle branch we get the de Broglie relation for single particle as $k_2/k_p \simeq v/v_p$, i.e., $k_2 \simeq p/\hbar$, where we have used the definition $v_p = \hbar k_p/m$. in the same limit from the wave branch one gets $k_1 \simeq 0$. Note that for the arbitrary value of the beam speed one obtains a dual lengthscale de Broglie relation. These lengscales correspond to single particle and collective excitations in the beam propagation.

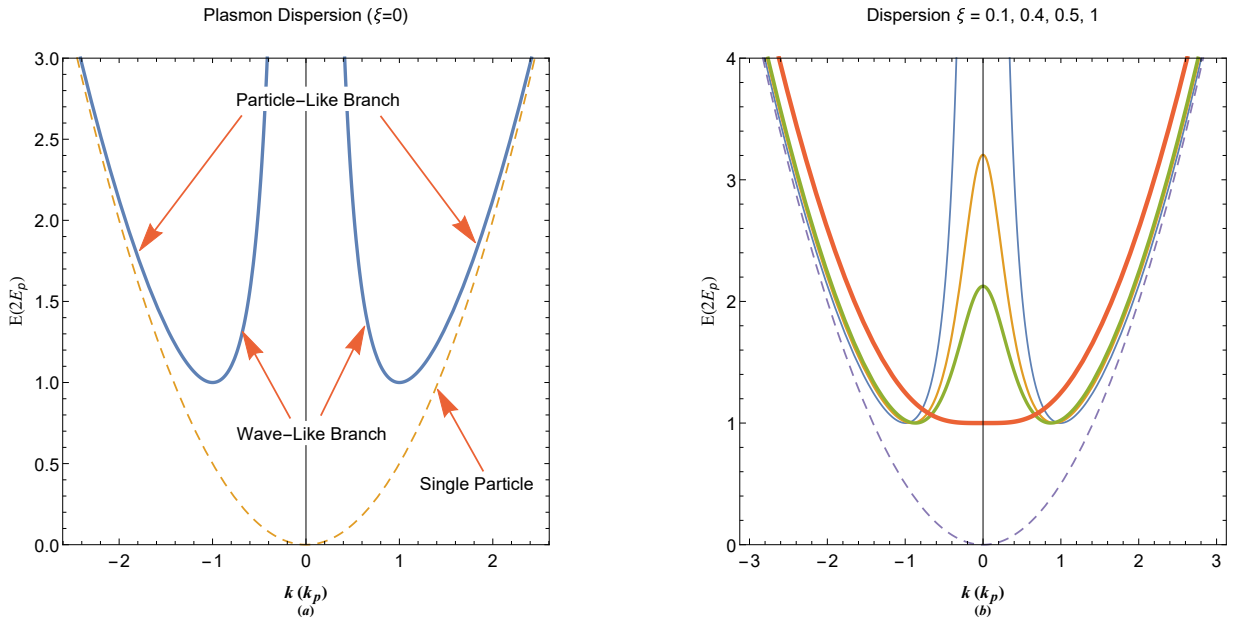

FIG. 1: (a) Energy dipersion curve for plasmon excitations in the absence of charge screening effect. The dashed curve indicates the standard parabolic free electron energy dispersion. (b) The plasmon energy dispersion in the presense of charge screening effect for different values of screening parameter. The thickness varies according to the value of changed parameter in plot (b).

IV. CHARGE SCREENING AND MATTER WAVE INSTABILITIES

Amplitudes of the solutions (12) are nonphysically divergent at resonant points. The later aspect is shown to be due to the resonant scattering and is better described by a generalized pseudodamped driven plasmon model in which the damping term represents the charge screening effect [81]

$$\frac{d^2\Psi(x)}{dx^2} + 2\xi\frac{d\Psi(x)}{dx} + \Phi(x) + 2E_k\Psi(x) = U_0\cos(k_d x), \tag{15a}$$

$$\frac{d^2\Phi(x)}{dx^2} + 2\xi\frac{d\Phi(x)}{dx} - \Psi(x) = 0, \tag{15b}$$

where $\xi = K/k_p$ with $\xi^2 = (E_p/2)\partial n/\partial\mu = (1/2\theta)\mathrm{Li}_{1/2}\left[-\exp(\mu/\theta)\right]/\mathrm{Li}_{3/2}\left[-\exp(\mu/\theta)\right]$ in which $\theta = T/T_p$ ($T_p = \hbar\omega_p/k_B$) and $\mu = \mu_0/2E_p$ is the normalized screening parameter. The

general solution to (15) is given as follows

$$\Phi(x) = \Phi_{gd}(x) - \frac{\mathrm{U}_0 \mathrm{e}^{-\xi x}}{2\alpha\eta_1\eta_2}\left[\eta_1\left(k_d^2 - k_2^2\right)\cos(\beta_2 x) - \eta_2\left(k_d^2 - k_1^2\right)\cos(\beta_1 x)\right] + \tag{16a}$$

$$\frac{U_0 \mathrm{e}^{-\xi x}}{2\alpha\eta_1\eta_2}\left[\xi\eta_1\left(k_d^2 + k_2^2\right)\frac{\sin(\beta_2 x)}{\beta_2} - \xi\eta_2\left(k_d^2 + k_1^2\right)\frac{\sin(\beta_1 x)}{\beta_1}\right] + \frac{U_0}{\eta_1\eta_2}\times \tag{16b}$$

$$\left\{\left[\left(k_d^2 - k_1^2\right)\left(k_d^2 - k_2^2\right) - 4k_d^2\xi^2\right]\cos(k_d x) + 2k_d\xi\left(k_1^2 + k_2^2 - 2k_d^2\right)\sin(k_d x)\right\}, \tag{16c}$$

$$\Psi(x) = \Psi_{gd}(x) + \frac{U_0 \mathrm{e}^{-\xi x}}{2\alpha\eta_1\eta_2}\left[\eta_1 k_2^2\left(k_d^2 - k_2^2\right)\cos(\beta_2 x) - \eta_2 k_1^2\left(k_d^2 - k_1^2\right)\cos(\beta_1 x)\right] - \tag{16d}$$

$$\frac{U_0 \mathrm{e}^{-\xi x}}{2\alpha\eta_1\eta_2}\left[\xi\eta_1 k_2^2\left(k_d^2 + k_2^2\right)\frac{\sin(\beta_2 x)}{\beta_2} - \xi\eta_2 k_1^2\left(k_d^2 + k_1^2\right)\frac{\sin(\beta_1 x)}{\beta_1}\right] - \frac{U_0}{\eta_1\eta_2}\times \tag{16e}$$

$$\left\{\left[1 - \left(k_1^2 + k_2^2 - k_d^2\right)\left(k_d^2 + 4\xi^2\right)\right]k_d^2\cos(k_d x) + 2k_d\xi\left(1 + k_d^4 - 4\xi^2 k_d^2\right)\sin(k_d x)\right\}, \tag{16f}$$

where $\beta_1 = \sqrt{k_1^2 - \xi^2}$, $\beta_2 = \sqrt{k_2^2 - \xi^2}$, $\eta_1 = (k_d^2 - k_1^2)^2 + 4k_d^2\xi^2$ and $\eta_2 = (k_d^2 - k_2^2)^2 + 4k_d^2\xi^2$. The amplitude of the solutions (16) does not diverge but has two strong peaks at the resonant de Broglie wavenumbers. Some parts of the solution (16) is strongly damped away from the screening centers and the remaining stable parts may be written in the following part

$$\Phi_s(x) = \frac{U_0\cos(k_d x - \theta_\phi)}{\eta_1\eta_2}, \quad \theta_\phi = \arctan\left[\frac{2\xi k_d\left(k_1^2 + k_2^2 - 2k_d^2\right)}{\left(k_d^2 - k_1^2\right)\left(k_d^2 - k_2^2\right) - 4k_d^2\xi^2}\right], \tag{17a}$$

$$\Psi_s(x) = -\frac{U_0\cos(k_d x - \theta_\psi)}{\eta_1\eta_2}, \quad \theta_\psi = \arctan\left[\frac{2(\xi/k_d)\left(1 + k_d^4 - 4\xi^2 k_d^2\right)}{1 - \left(k_1^2 + k_2^2 - k_d^2\right)\left(k_d^2 + 4\xi^2\right)}\right]. \tag{17b}$$

It is clearly remarked that the stable solution propagates with the de Broglie wavelength $\lambda = h/p$ in space in which h is the planck constant. Also, the damped solution (16) gives rise to a new energy dispersion relation $E = [1 + (k^2 + \xi^2)^2]/2(k^2 + \xi^2)$. The variation of the new energy dispersion relation is shown in Fig. 1(b) for various values of the charge screening parameter. It is remarked that with increase in the value of screening parameter the wave branch of the dispersion diminishes and at the critical screening point $\xi = 1$ it totaly disappears. Therefore, for a given value of the plasmon energy this corresponds to only a particle-like de Broglie wavenumber below a critical plasmon energy, $E_{cr} = (1 + \xi^4)/2\xi^2$. Using the parabolic nonrelativistic energy relation $\epsilon = p^2/2m$ for average beam particles one arrives at the normalized de Broglie relation

$$k_{1,2} = \sqrt{\frac{\gamma^2 - \mu}{2} - \xi^2 \mp \sqrt{\frac{\left(\gamma^2 - \mu\right)^2}{4} - 1}}, \tag{18}$$

where the minus/plus sign correspond to the wave/particle de Broglie wavenumbers, respectively. The quantum de Brodlie wavenumber, k_d, has a value larger than that of the particle

branch of plasmon excitation. These two wavenumbers however become identical as the beam speed approaches infinity. The normalized relative de Broglie wavenumber difference $\delta k = (k_d - k_2)/k$ may be written as

$$\frac{\delta k}{k} = 1 - \sqrt{\frac{1-\mu/\gamma^2}{2} - \frac{\xi^2}{\gamma^2} + \sqrt{\frac{\left(1-\mu/\gamma^2\right)^2}{4} - \frac{1}{\gamma^4}}}. \tag{19}$$

The equation (18) can be written as $k_{1,2} = \chi_{1,2}(p/\hbar)$ in which the wave-like and particle-like de Broglie coefficients $\chi_{1,2}$ are given as

$$\chi_{1,2}(\mu,\theta,E_k) = \sqrt{\frac{1}{2}\left(1-\frac{\mu}{E_K}\right) - \frac{\mathrm{Li}_{1/2}\left[-\exp(\mu/\theta)\right]}{2\theta E_k \mathrm{Li}_{3/2}\left[-\exp(\mu/\theta)\right]} \mp \sqrt{\frac{1}{4}\left(1-\frac{\mu}{E_K}\right)^2 - \frac{1}{E_K^4}}}, \tag{20}$$

in which E_K is the nonrelativistic normalized kinetic energy of the beam to the plasmon energy. Note that for relativistic beam E_K can not be simply replaced with the relativistic kinetic energy due to the fact that nonrelativistic hydrodynamic model has been used in current research. Note also that in the classical beam limit, $\mu/\theta \ll -1$, we have $\mathrm{Li}_\nu[-\exp(\mu/\theta)] \approx -\exp(\mu/\theta)$ and $\mu_0 \simeq 0$. On the other hand, in the quantum beam limit $\mu/\theta \gg 1$, one has $\lim_{\mu/\theta\to\infty} \mathrm{Li}_\nu[-\exp(\mu/\theta)] = -(\mu/\theta)^\nu/\Gamma(\nu+1)$ and $\mu_0 \simeq E_F$ in which E_F is the Fermi energy of the electron fluid. It is clearly evident that in the classical beam limit, $\mu_0 \ll E_p$ and $E_K \gg E_p$, we have $\chi_{1,2} = \{0,1\}$, as expected for the single electron wavenumbers.

The complex form of wave-like and particle-like de Broglie wavenumbers may be written as $k_1 = k_r - ik_i$ and $k_2 = k_r + ik_i$, the real and imaginary parts for $\gamma < \sqrt{\mu}$ and $\xi < 1$ are given as

$$k_r = \sqrt[\frac{1}{4}]{\left(\frac{\gamma^2-\mu}{2} - \xi^2\right)^2 - \left[\frac{\left(\gamma^2-\mu\right)^2}{4} - 1\right]} \cos\left\{\frac{1}{2}\tan^{-1}\left[\frac{\sqrt{4-\left(\gamma^2-\mu\right)^2}}{2\xi^2-\gamma^2+\mu}\right]\right\}, \tag{21a}$$

$$k_i = \sqrt[\frac{1}{4}]{\left(\frac{\gamma^2-\mu}{2} - \xi^2\right)^2 - \left[\frac{\left(\gamma^2-\mu\right)^2}{4} - 1\right]} \sin\left\{\frac{1}{2}\tan^{-1}\left[\frac{\sqrt{4-\left(\gamma^2-\mu\right)^2}}{2\xi^2-\gamma^2+\mu}\right]\right\}. \tag{21b}$$

Note that in this regime the real and imaginary parts of the wave- and particle-like branches have the same magnitude but the imaginary parts have opposite signs. On the other hand for $\sqrt{\mu} < \gamma < \sqrt{\mu+2}$ and $\xi < 1$ with $k_1 = k_r - ik_i$ and $k_2 = k_r + ik_i$, the real/imaginary

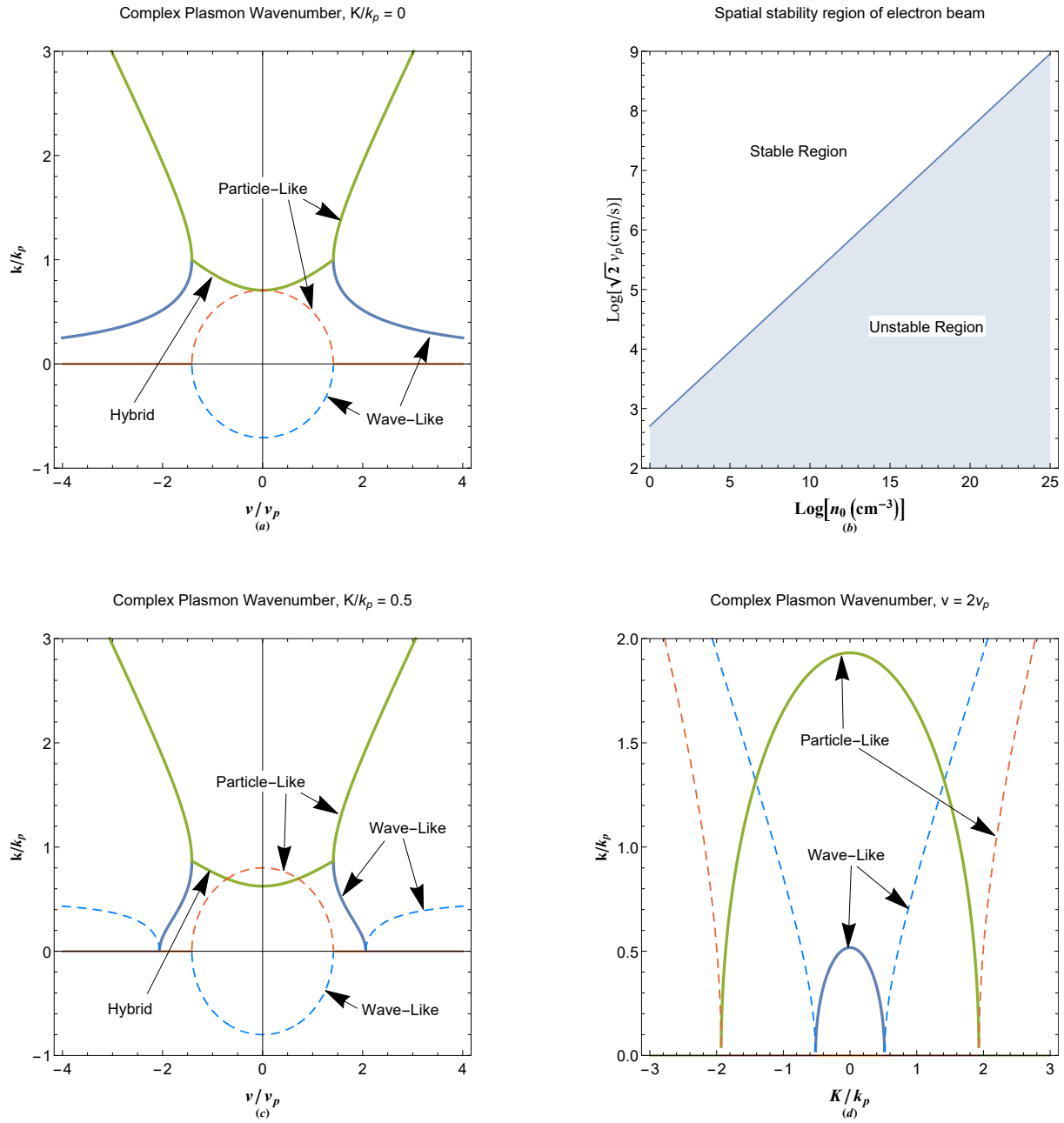

FIG. 2: (a) Complex wavenumbers of plasmon excitations for plasmon excitation in a classical dilute electron beam. (b) The beam propagation stability region in terms of the beam electron density. (c) Effect of charge screening on the stability of wave-like and particle-like de Broglie oscillations in an electron beam. (d) Variations in real and imaginary parts of de Broglie matter waves with changes in the screening parameter.

component reads

$$k_r = \sqrt[\frac{1}{4}]{\left(\frac{\gamma^2-\mu}{2}-\xi^2\right)^2-\left[\frac{(\gamma^2-\mu)^2}{4}-1\right]}\sin\left\{\frac{1}{2}\tan^{-1}\left[\frac{\sqrt{4-(\gamma^2-\mu)^2}}{2\xi^2-\gamma^2+\mu}\right]\right\}, \tag{22a}$$

$$k_i = -\sqrt[\frac{1}{4}]{\left(\frac{\gamma^2-\mu}{2}-\xi^2\right)^2-\left[\frac{(\gamma^2-\mu)^2}{4}-1\right]}\cos\left\{\frac{1}{2}\tan^{-1}\left[\frac{\sqrt{4-(\gamma^2-\mu)^2}}{\gamma^2+\mu-2\xi^2}\right]\right\}. \tag{22b}$$

Moreover, for $\sqrt{\mu+2} < \gamma < \sqrt{\xi^2+\xi^{-2}+\mu}$ and $\xi < 1$ both of k_1 and k_2 are purely real with the components

$$k_{1i} = 0, \quad k_{1r} = \sqrt{\frac{\gamma^2-\mu}{2}-\xi^2-\sqrt{\frac{(\gamma^2-\mu)^2}{4}-1}}, \tag{23a}$$

$$k_{2i} = 0, \quad k_{2r} = \sqrt{\frac{\gamma^2-\mu}{2}-\xi^2+\sqrt{\frac{(\gamma^2-\mu)^2}{4}-1}}. \tag{23b}$$

Finally, for $\gamma > \sqrt{\xi^2+\xi^{-2}+\mu}$ and $\xi < 1$, the particle-like branch is purely real and the wave-like branch is purely imaginary the components of which are given as

$$k_{1r} = 0, \quad k_{1i} = \sqrt{\sqrt{\frac{(\gamma^2-\mu)^2}{4}-1}-\left(\frac{\gamma^2-\mu}{2}\right)+\xi^2}, \tag{24a}$$

$$k_{2i} = 0, \quad k_{2r} = \sqrt{\frac{\gamma^2-\mu}{2}-\xi^2+\sqrt{\frac{(\gamma^2-\mu)^2}{4}-1}}. \tag{24b}$$

However, the case $\xi > 1$ is not studied here. Variations of the de Broglie wavenumbers in terms of normalized beam speed is shown in Fig. 2(a) in the absence of screening, $\xi = 0$ and for classical dilute beam $\mu_0 \ll E_p$. It is clearly remarked that below a critical velocity $v_{cr} = \sqrt{2}v_p$ the wavenumbers are both complex. Above this critical beam speed the wavenumbers are real and the particle-like de Broglie wavenumber increases rapidly with increase in the beam speed while the wave-like wavenumber decreases slowly. The imaginary component of the wavenumbers below the critical point indicates spatial damping or growing of the wave amplitude depending on its sign. It is remarked from Fig. 2(a) (22) that below the critical beam speed amplitude of the wave-like branch grows while that of the particle-like damps and this effect enhances as the beam speed decreases towards zero. The real part of the two branches coincide at the damping/growing regime and it decreases as the beam speed decreases. The stable/unstable regimes of electron beam propagation in terms of the

beam density is depicted in Fig. 2(b). It is remarked that the stable beam speed region rapidly increase as the electron beam number density increases. This plot is only valid for the classical beam density since we have plotted the figure assuming $\mu_0 \ll E_p$. A better figure may be produced using the generalized relation $v_{cr} = v_p\sqrt{\mu+2}$ in which $\mu = \mu_0/E_p$ is the density and temperature dependent normalized equilibrium chemical potential.

Figure 2(c) shows de Broglie wavenumber components for given value of the screening parameter $\xi = 0.5$ for a classical dilute beam $\mu = 0$. It is remarked that the introduction of charge screening for beam electrons leads to an upper limit instability of the wave-like branch beyond a critical beam speed. It is found that both the beam oscillation components are always spatially stable when the speed varies in the range $\sqrt{\mu+2} < v/v_p < \sqrt{\mu+\xi^{-2}+\xi^2}$. Note that when $\xi = 1$ for th ecomplete screening case the stable range completely vanishes. It is further revealed that the charge screening leads to increase/decrease of the imaginary/real part of the de Broglie wavenumber in the range $v > v_p\sqrt{\mu+2}$. Note that the screening parameter ξ is a function of the normalized chemical potential and electron temperature. It is to be noted that the upper-limit instability of wave-like branch is damping type and increases with increase in the beam speed. The variation of beam stability is depicted in Fig. 2(d) in terms of the change in the screening parameter for a given value of fractional beam speed $v/v_p = 2$. It is seen that the wave-like de Broglie branch becomes unstable at lower value of the screening parameter compared to that of the particle-like branch. Also, the real/imaginary component of wave-like branch are always lower/higher than that for the particle branch in the whole range of screening parameter, ξ.

Figure 3 shows the real and imaginary parts of matter waves for an electron beam in Aluminium and Silver metals. Aluminium has the Fermi energy of $\mu_0 \simeq 11.7$eV and the plasmon energy of $E_p \simeq 15$eV. On the other hand, these energies for Silver are $\mu_0 \simeq 5.49$eV and $E_p \simeq 3.76$eV, respectively. As remarked by comparing the plots 3(a) and 3(b) in the absence of charge screening there is slight difference between them. In the Silver the unstable range extends to higher value of the fractional parameter v/v_p as compared to the Aluminium due to the relatively smaller chemical potential of the Silver. Moreover, the magnitude of imaginary/real part of the de Broglie wavenumber in Silver is slightly higher/lower compared to that in Aluminium. It is however concluded that, a beam of electron with a given under critical speed penetrates more distance or has a longer penetration depth in Aluminium as compared to the Silver metal. On the other hand, plots 3(c) and 3(d) shows the de Broglie

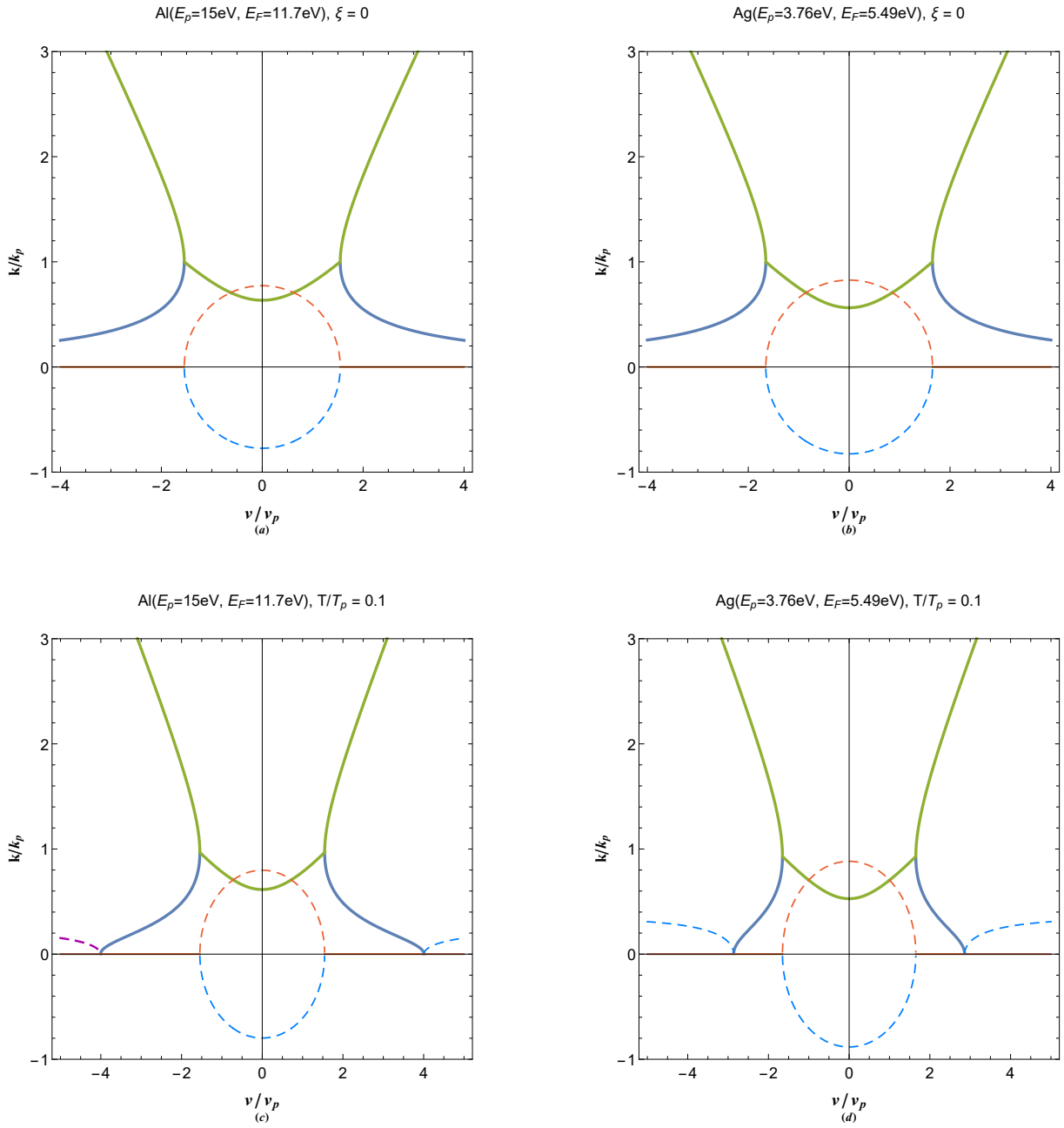

FIG. 3: The matter wave instability in (a) Aluminium and (b) Silver metals in the absence of the charge screening effect. Complex wavenumber of de Broglie's matter waves for (a) Aluminium and (b) Silver in the presence of the charge screening effect at the fractional temperature $\theta = 0.1$.

instability in these metal in the presence of screening which has corresponding parameters $\xi_{Al} = 0.25317$ and $\xi_{Ag} = 0.36951$ at the temperature $\theta = T/T_p = 0.1$. It is seen that in Silver in $\theta = 0.1$ the wave-like branch of the de Broglie wave damps at much lower fractional speed v/v_p value compared to that in Aluminium. It is however confirmed by comparing

these plots that the speed range of stability for wave-like plasmon branch in Aluminium is greatly higher compared to the Silver metal.

V. ELECTRON BEAM-LATTICE INTERACTION

For our final purpose we would like to investigate the effect of de Broglie pseudoresonance on Bragg scattering in a one dimensional periodic density structure. In order to model such effect we consider the following coupled pseudoforce system

$$\frac{d^2\Psi(x)}{dx^2} + \Phi(x) + 2E_k\Psi(x) = U_0\cos(k_d x), \tag{25a}$$

$$\frac{d^2\Phi(x)}{dx^2} - \Psi(x) = U_g\cos(Gx), \tag{25b}$$

in which U_g is the lattice potential as normalized to the plasmon energy and $G = 2\pi/a$ is the reciprocal lattice vector and a is lattice constant as normalized to the plasmon wavelength, λ_p. The general solution this system may be written as follows

$$\Phi(x) = \Phi_g(x) + \frac{U_0\cos(k_d x)}{(k_d^2 - k_1^2)(k_d^2 - k_2^2)} - \frac{U_g(G^2 - k_1^2 - k_2^2)\cos(Gx)}{(G^2 - k_1^2)(G^2 - k_2^2)} - \tag{26a}$$

$$\left[\frac{U_0}{(k_d^2 - k_1^2)} + \frac{U_g k_2^2}{(G^2 - k_1^2)}\right]\frac{\cos(k_1 x)}{2\alpha} - \left[\frac{U_0}{(k_d^2 - k_2^2)} + \frac{U_g k_1^2}{(G^2 - k_2^2)}\right]\frac{\cos(k_2 x)}{2\alpha}, \tag{26b}$$

$$\Psi(x) = \Psi_g(x) - \frac{U_0 k_d^2\cos(k_d x)}{(k_d^2 - k_1^2)(k_d^2 - k_2^2)} - \frac{U_g\cos(Gx)}{(G^2 - k_1^2)(G^2 - k_2^2)} + \tag{26c}$$

$$\left[\frac{U_0 k_1^2}{(k_d^2 - k_1^2)} + \frac{U_g}{(G^2 - k_1^2)}\right]\frac{\cos(k_1 x)}{2\alpha} + \left[\frac{U_0 k_2^2}{(k_d^2 - k_2^2)} + \frac{U_g}{(G^2 - k_2^2)}\right]\frac{\cos(k_2 x)}{2\alpha}. \tag{26d}$$

The solution constants $\Phi(0)$ and $\Psi(0)$ may be fixed using the periodic condition of the lattice structure by the following boundary condition

$$\Phi(0) = \Phi(a), \quad \left.\frac{d\Phi(x)}{dx}\right|_{x=0} = \left.\frac{d\Phi(x)}{dx}\right|_{x=a}, \tag{27a}$$

$$\Psi(0) = \Psi(a), \quad \left.\frac{d\Psi(x)}{dx}\right|_{x=0} = \left.\frac{d\Psi(x)}{dx}\right|_{x=a}. \tag{27b}$$

The lattice wavefunction solution is

$$\Phi_n(x) = \frac{U_0\cos(k_d x)}{(k_d^2 - k_1^2)(k_d^2 - k_2^2)} - \frac{U_g(n^2G^2 - k_1^2 - k_2^2)\cos(nGx)}{(n^2G^2 - k_1^2)(n^2G^2 - k_2^2)}, \tag{28a}$$

$$\Psi_n(x) = -\frac{U_0 k_d^2\cos(k_d x)}{(k_d^2 - k_1^2)(k_d^2 - k_2^2)} - \frac{U_g\cos(nGx)}{(n^2G^2 - k_1^2)(n^2G^2 - k_2^2)}, \tag{28b}$$

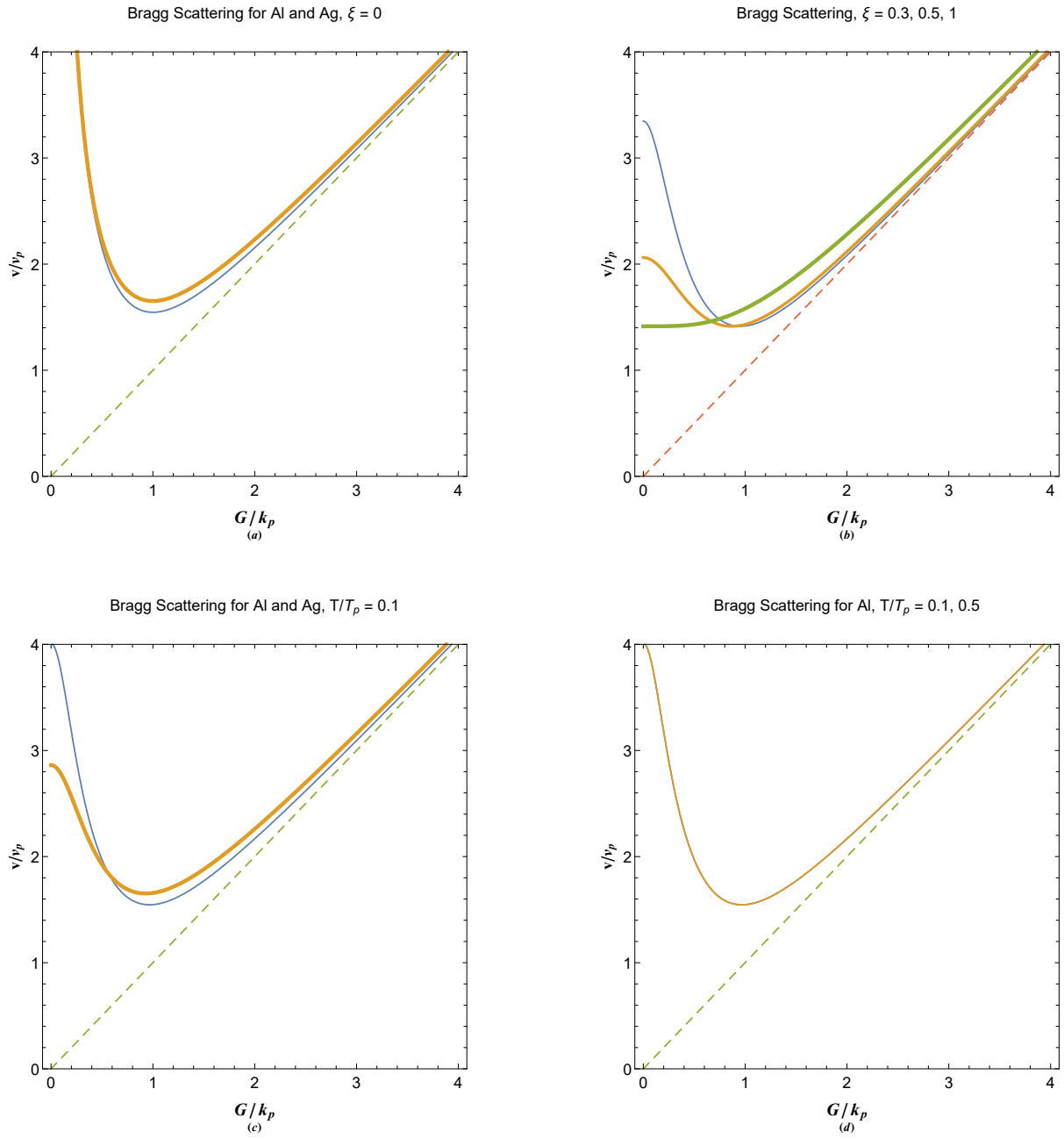

FIG. 4: (a) The resonant Bragg scattering by de Broglie's matter waves for Aluminium (thin curve) and Silver (thick curve). (b) Effect of charge screening on the resonant Bragg scattering. The thickness of curves in this plot indicates incarese in the value of varied screening parameter. (c) Bragg scattering for Aluminium (thin curve) and Silver (thick curve) in the presence of charge screening effect at fractional temperature $\theta = 0.1$. (d) Effect of fractional electron fluid temperature θ on Bragg scattering in Aluminium.

where n is an arbitrary integer indexing the discrete reciprocal lattice vector, G. It is clearly remarked that the solutions (28) has four resonant elements. These are of course doubly degenerate resonant conditions reduced to the generalized Bragg condition $k_d = nG$ for which the de Broglie's wavenumbers of a beam entering the lattice are defined through the conditions $k_d = k_1$ and $k_d = k_2$ discussed previously. It is seen that de Broglie wavelengths of the beam resonantly interact with the lattice periodicity through the generalized Bragg condition. The resonant beam speed components are given through the relation $\gamma = \sqrt{(n^2G^2 + \xi^2)^{-1} + (n^2G^2 + \xi^2 + \mu)}$. Figure 4(a) depicts the variations of the fractional beam speed $\gamma = v/v_p$ in Al and Ag metals in terms of the first ($n = 1$) reciprocal lattice vector in the absence of charge screening. It is remarked that for beam speed higher than the critical speed $v_{cr} = v_p\sqrt{\mu + 2}$ two quantized resonant Bragg scattering corresponding to the wave-like and particle-like dual lengthscales of the beam exist. For beam speed below this critical value the Bragg interaction does not take place due to the de Broglie instabilities. It is further remarked that for very energetic beam the particle-like branch interacts resonantly with the lattice vector at point $v/v_p \simeq G$ indicated by the dashed line. In Fig. 4(b) depicts the effect of charge screening on resonant beam-lattice interaction for different values of the screening parameter. It is seen that there is a cut-off value for the wave-like Bragg interaction in the presence of the charge screening. For the critical value of $\xi = 1$ the beam-lattice Bragg interaction only becomes limited to the particle-like channel. Figure 4(c) shows the Bragg interaction for Al and Ag metals in the presence of charge screening at fractional temperature $\theta = 0.1$. It is evident that the wave-like branch cut-off speed is relatively higher in Aluminium as compared to Silver. Figure 4(d), on the other hand, reveals the insignificant effect of temperature on the Bragg interaction pattern.

VI. CONCLUSION

The Schrödinger-Poisson system derived from the quantum hydrodynamic model was reduced to the appropriate coupled driven pseudoforce equation in order to describe the propagation of an electron beam with arbitrary degree of degeneracy. The fundamental de Broglie matter wave equation of quantum mechanics is discovered to be due to resonant interaction of particle-like plasmonic oscillation branch with the constant electron drift in the beam. A generalized dual scalelength de Broglie matter wave relation is obtained

through which various wave-particle type instabilities were discussed. We also investigated the important effects such as the charge screening and periodic lattice density effect on these new phenomenon. Current investigation may further elucidate the underlying nature of less understood particle waves as a fundamental building block of the quantum theory and interaction of such waves with real material.

---

[1] F. F. Chen, Introduction to Plasma Physics and Controlled Fusion, 2nd ed. (Plenum Press, New York, London, 1984).

[2] N. A. Krall and A. W. Trivelpeice, "Principles of Plasma Physics", (San francisco Press, San francisco 1986).

[3] P. G. Drazin and R. S. Johnson, "Solitons: an introduction", Cambridge Texts in Applied Mathematics, Cambridge University Press, (l993)

[4] L. Stenflo, Phys. Scripta 14, 320(1976).

[5] L. Stenflo, and N. L. Tsintsadze, Astrophys. Space Sci. 64, 513(1979).

[6] L. Stenflo, Phys. Scripta 23, 779(1981).

[7] L. Stenflo and P. K. Shukla, Phys. Plasmas 6, 1382(1999).

[8] S. Ichimaru, Rev. Mod. Phys. **54**, 1017 (1982).

[9] S. Ichimaru, H. Iyetomi, and S. Tanaka, Phys. Rep. **149**, 91 (1987).

[10] S. Ichimaru, *Statistical Physics: Condensed Plasmas* (Addison Wesely, New York, 1994).

[11] K. Sturm, Z. Naturforsch. **48a**, 233-242(1993).

[12] Young-Dae Jung, Phys. Plasmas **8**, 3842 (2001); doi.org/10.1063/1.1386430

[13] Young-Dae Jung, EPL **102**, 4(2013).

[14] Young-Dae Jung, APS **695**, 2(2009).

[15] S. Son, Phys. Plasmas **21**, 034502 (2014); doi.org/10.1063/1.4865826

[16] Ch. Rozina, S. Ali, N. Maryam, and N. L. Tsintsadze, Phys. Plasmas 25, 093302 (2018); doi.org/10.1063/1.5031423

[17] L. B. Zhao and Y. K. Ho, Phys. Plasmas **11**, 1695 (2004).

[18] Zh. A. Moldabekov, P. Ludwig, J.-P. Joost, M. Bonitz, and T. S. Ramazanov, Contrib. Plasma Phys., No. **X**, 1 (2015); doi:10.1002/ctpp.201400105

[19] W. Hong and Y. D. Jung, Phys. Plasmas **3**, 2457 (1996).

[20] Y. D. Jung, Phys. Fluids B **5**, 3432 (1993); Phys. Plasmas **2**, 332 (1995);

[21] Y. D. Jung, ibid. **2**, 987 (1995); Y. D. Jung, ibid. **5**, 3781 (1998); Y. D. Jung, ibid. **5**, 4456 (1998).

[22] J. S. Yoon and Y. D. Jung, Phys. Plasmas **3**, 3291 (1996).

[23] B. Eliasson and M. Akbari-Moghanjoughi, Phys. Lett. A, **380**, 2518(2016); doi.org/10.1016/j.physleta.2016.05.043

[24] A. C. H. Yu and Y. K. Ho, Phys. Plasmas **12**, 043302 (2005).

[25] S. Sahoo and Y. K. Ho, Phys. Plasmas **13**, 063301 (2006).

[26] S. Kar and Y. K. Ho, Phys. Plasmas **15**, 013301 (2008).

[27] S. Paul and Y. K. Ho, Phys. Plasmas **16**, 063302 (2009).

[28] S. Paul and Y. K. Ho, Phys. Plasmas **15**, 073301 (2008).

[29] S. Paul and Y. K. Ho, Phys. Rev. A **78**, 042711 (2008).

[30] S. Paul and Y. K. Ho, Phys. Plasmas **17**, 082704 (2010).

[31] S. Paul and Y. K. Ho, Comput. Phys. Commun. **182**, 130 (2011).

[32] A. Soylu and I. Boztosun, Physica B **396**, 150 (2007).

[33] A. Soylu, O. Bayrak, and I. Boztosun, J. Phys. A **41**, 065308 (2008).

[34] M. Akbari-Moghanjoughi, Phys. Plasmas, **26**, 072106 (2019); doi.org/10.1063/1.5097144

[35] C. Kittel, Introduction to Solid State Physics, (John Wiely and Sons, New York, 1996), 7th ed.

[36] N. W. Ashcroft and N. D. Mermin, Solid State Physics (Saunders College Publishing, Orlando, 1976).

[37] C. Hu, Modern Semiconductor Devices for Integrated Circuits (Prentice Hall, Upper Saddle River, New Jersey, 2010) 1st ed.

[38] K. Seeger, Semiconductor Physics (Springer, Berlin, 2004) 9th ed.

[39] L. C. Andreani, Physics Today **67**, 53(2014); doi.org/10.1063/PT.3.2386.

[40] P. A. Markovich, C.A. Ringhofer, and C. Schmeister, Semiconductor Equations (Springer, Berlin, 1990).

[41] H. Haug and S. W. Koch, "Quantum theory of the optical and electronic properties of semiconductors", World Scientific, 2004,

[42] C. Gardner, SIAM, J. Appl. Math. **54** 409(1994).

[43] G. Manfredi, Phys. Plasmas **25**, 031701(2018); https://doi.org/10.1063/1.5026653

[44] S. A. Maier, Plasmonics: Fundamentals and Aplications, Springer Science Business Media LLC (2007).

[45] A. D. Yofee, Adv. Phys., **42**, 173-262(1993), DOI: 10.1080/00018739300101484

[46] F. Haas, *Quantum Plasmas: An Hydrodynamic Approach* (Springer, New York, 2011).

[47] Giovanni Manfredi, arXiv:1912.06549 [physics.plasm-ph]

[48] E. Madelung, Z. Phys., 40 322(1926).

[49] E. Fermi and E. Teller, Phys. Rev. **72**, 399 (1947).

[50] F. Hoyle and W. A. Fowler, Astrophys. J. **132**, 565(1960).

[51] S. Chandrasekhar, "*An Introduction to the Study of Stellar Structure*", The University of Chicago Press, Chicago (1939).

[52] D. Bohm and D. Pines, Phys. Rev. **92** 609(1953).

[53] Bohm, D. Phys. Rev. **85**, 166179 (1952).

[54] Bohm, D. Phys. Rev. **85**, 180193 (1952).

[55] D. Pines, Phys. Rev. **92** 609(1953).

[56] P. Levine and O. V. Roos, Phys. Rev, **125** 207(1962).

[57] Y. Klimontovich and V. P. Silin, in Plasma Physics, edited by J. E. Drummond (McGraw-Hill, New York, 1961).

[58] J. Lindhard, Kgl. Danske Videnskab. Selskab, Mat.-Fys. Medd. **28**, (1954).

[59] F. Stern, Phys. Rev. Lett. **18**, 546 (1967).

[60] A. L. Fetter and J. D. Walecka, Quantum Theory of Many-Particle Systems,. McGraw-Hill 1971.

[61] G. D. Mahan, Many-particle physics, 2nd edition, chapter 5 (Plenum press, New York, (1990).

[62] P. K. Shukla and B. Eliasson, Phys. Rev. Lett. **99**, 096401(2007).

[63] L Stenflo Phys. Scr. **T50** 15(1994).

[64] P. K. Shukla, B. Eliasson, and L. Stenflo Phys. Rev. E **86**, 016403(2012).

[65] G. Brodin and M. Marklund, New J. Phys. **9**, 277(2007).

[66] M. Marklund and G. Brodin, Phys. Rev. Lett. **98**, 025001(2007).

[67] N. Crouseilles, P. A. Hervieux, and G. Manfredi, Phys. Rev. B **78**, 155412 (2008).

[68] Z. Moldabekov, Tim Schoof, Patrick Ludwig, Michael Bonitz, and Tlekkabul Ramazanov, Phys. Plasmas, **22**, 102104(2015); doi.org/10.1063/1.4932051

[69] L. Stanton and M. S. Murillo, Phys. Rev. E **91**, 033104(2015).

[70] J. Hurst, K. L. Simon, P. A. Hervieux, G. Manfredi and F. Haas, Phys. Rev. B **93**, 205402(2016).

[71] F. Haas, G. Manfredi, P. K. Shukla, and P.-A. Hervieux, Phys. Rev. B, **80**, 073301 (2009).

[72] B. Eliasson and P. K. Shukla, Phys. Scr. **78**, 025503 (2008).

[73] Hwa-Min Kim and Young-Dae Jung, EPL, **79** 25001(2007).

[74] G. Manfredi and F. Haas, Phys. Rev. B **64**, 075316 (2001);

[75] M. Akbari-Moghanjoughi, Phys. Plasmas, **26**, 012104 (2019); doi.org/10.1063/1.5078740

[76] M. Akbari-Moghanjoughi, Phys. Plasmas, **26**, 022110 (2019); doi.org/10.1063/1.5087201

[77] M. Akbari-Moghanjoughi, Phys. Plasmas, **26**, 022111 (2019); doi.org/10.1063/1.5083150

[78] M. Akbari-Moghanjoughi, Phys. Plasmas, **26**, 052104 (2019); doi.org/10.1063/1.5080347

[79] M. Akbari-Moghanjoughi, Phys. Plasmas, **26**, 062105 (2019); doi.org/10.1063/1.5090366

[80] M. Akbari-Moghanjoughi, Phys. Plasmas, **26**, 062110 (2019); doi.org/10.1063/1.5098054

[81] M. Akbari-Moghanjoughi, Phys. Plasmas, **26**, 112102 (2019); doi.org/10.1063/1.5123621

[82] Z. Merali, Nat. News, **521**, 278(2015); doi:10.1038/521278a

[83] D. Bohm, Phys. Rev. **85** 166(1952); doi:10.1103/PhysRev.85.166

[84] Mahdi Atiq, Mozafar Karamian, Mehdi Golshani, Annales de la Fondation Louis de Broglie, **34**, 67(2009).

[85] L. de Broglie, Ann. Fondation 12, 4 (1987); available at aflb.ensmp.fr/AFLB-classiques/aflb124p001.pdf